

Panel data analysis via mechanistic models

Carles Bretó and Edward L. Ionides

Department of Statistics, University of Michigan

and

Aaron A. King*

Department of Ecology and Evolutionary Biology, University of Michigan

January 18, 2018

Abstract

Panel data, also known as longitudinal data, consist of a collection of time series. Each time series, which could itself be multivariate, comprises a sequence of measurements taken on a distinct unit. Mechanistic modeling involves writing down scientifically motivated equations describing the collection of dynamic systems giving rise to the observations on each unit. A defining characteristic of panel systems is that the dynamic interaction between units should be negligible. Panel models therefore consist of a collection of independent stochastic processes, generally linked through shared parameters while also having unit-specific parameters. To give the scientist flexibility in model specification, we are motivated to develop a framework for inference on panel data permitting the consideration of arbitrary nonlinear, partially observed panel models. We build on iterated filtering techniques that provide likelihood-based inference on nonlinear partially observed Markov process models for time series data. Our methodology depends on the latent Markov process only through simulation; this plug-and-play property ensures applicability to a large class of models. We demonstrate our methodology on a toy example and two epidemiological case studies. We address inferential and computational issues arising for large panel datasets.

Keywords: longitudinal data; particle filter; sequential Monte Carlo; likelihood; nonlinear dynamics.

*This research was supported by National Science Foundation grant DMS-1308919 and National Institutes of Health grants U54-GM111274, U01-GM110712 and R01-AI101155.

1 Introduction

Analyzing time series data on a collection of related units provides opportunities to study aspects of dynamic systems—their replicability, or dependence on properties of the units—that cannot be revealed from measurements on a single unit. The units might be individual humans or animals, in an observational or experimental study. The units might also be spatial locations, giving a panel representation of spatiotemporal data. As a consequence of advances in data collection, scientists investigating dynamic systems have growing capabilities to obtain measurements of increasing length on increasingly many units. Statistical investigation of such data, known as panel data analysis, is therefore playing a growing role in the scientific process.

Mechanistic modeling of a dynamic system involves writing down equations describing the evolution of the system through time. Time series analysis using mechanistic models involves determining whether the model provides an adequate description of the system, and if so, identifying plausible values for unknown parameters (Bretó et al., 2009). Stochasticity, nonlinearity and noisy incomplete observations are characteristic features of many systems in the biological and social sciences (Bjørnstad and Grenfell, 2001; Dobson, 2014). Monte Carlo inference approaches have been developed that are effective for general classes of models with these properties; such methods include iterated filtering (Ionides et al., 2006, 2015), particle Markov chain Monte Carlo (Andrieu et al., 2010) and synthetic likelihood (Wood, 2010). All these inference algorithms obtain their general applicability by enjoying the plug-and-play property, that is, they interface with the dynamic model only through simulation (Bretó et al., 2009; He et al., 2010). However, these methodologies do not address the particular structure of panel models and the high-dimensional nature of panel data. Therefore, new methodology is required to analyze panel data when there is a need to consider models outside the linear, Gaussian paradigm. We proceed by building on the iterated filtering approach of Ionides et al. (2015) to derive a panel iterated filtering likelihood maximization algorithm. The panel iterated filtering algorithm, an associated convergence theorem, and a software implementation equipped with an appropriate domain-specific modeling language, all extend the existing theory and practice of iterated filtering.

Across the broad applications of nonlinear partially observed stochastic dynamic models for time series analysis (Douc et al., 2014) one can anticipate many situations where multiple time series are available and give rise to the structure of panel data. In particular, panel data on dynamic systems arises in pharmacokinetics (Donnet and Samson, 2013), molecular biology (Chen et al., 2016), infectious disease transmission (Cauchemez et al., 2004; Yang et al., 2010, 2012), and microeconomics (Heiss, 2008; Bartolucci et al., 2012; Mesters and Koopman, 2014). Our methodology differs from these analyses by providing plug-and-play likelihood-based inference applicable to general nonlinear, non-Gaussian models. This scope of applicability also sets our goals apart from the extensive panel methodology literature building on a linear regression framework (e.g., Hsiao, 2014).

In Section 2 we present a basic panel iterated filtering algorithm, and in Section 3 we prove its convergence under appropriate regularity conditions. An issue arising for large panel datasets is scalability of statistical methodology, and we develop three techniques to

address this issue in Sections 4.1, 4.2 and 4.3. These scaling techniques are illustrated on a toy example in Section 4.4. Two scientifically motivated examples follow: modeling the transmission of polio in Section 5, and dynamic variation in human sexual contact rates in Section 6. Section 7 is a concluding discussion.

2 Inference methodology: panel iterated filtering (PIF)

Units of a panel are labeled $\{1, 2, \dots, U\}$, which we write as $1:U$. The N_u measurements collected on unit u are written as $y_{u,1:N_u}^* = \{y_{u,1}^*, \dots, y_{u,N_u}^*\}$ where $y_{u,n}^*$ is collected at time $t_{u,n}$ with $t_{u,1} < t_{u,2} < \dots < t_{u,N_u}$. These data are considered fixed and modeled as a realization of an observable stochastic process $Y_{u,1:N_u}$. This observable process is constructed to be dependent on a latent Markov process $\{X_u(t), t_{u,0} \leq t \leq t_{u,N_u}\}$, for some $t_{u,0} \leq t_{u,1}$. Further requiring that $\{X_u(t)\}$ and $\{Y_{u,i}, i \neq n\}$ are independent of $Y_{u,n}$ given $X_u(t_{u,n})$, for each $n \in 1:N_u$, completes the structure required for a partially observed Markov process (POMP) model for unit u . If all units are modeled as independent, the model is called a PanelPOMP. We are primarily interested in the latent process at the observation times, so we write $X_{u,n} = X_u(t_{u,n})$. We suppose that $X_{u,n}$ and $Y_{u,n}$ take values in arbitrary spaces \mathbb{X}_u and \mathbb{Y}_u respectively. We suppose that the joint density of $X_{u,0:N_u}$ and $Y_{u,1:N_u}$ exists, with respect to some suitable measure, and is written as $f_{X_{u,0:N_u} Y_{u,1:N_u}}(x_{u,0:N_u}, y_{u,1:N_u}; \theta)$, with dependence on an unknown parameter $\theta \in \Theta \subset \mathbb{R}^{\dim(\Theta)}$. Each component of the vector θ may affect one, several or all units. This framework encompasses fixed effects (discussed in Section 4.2) and random effects (discussed in Section 7). The transition density $f_{X_{u,n}|X_{u,n-1}}(x_{u,n} | x_{u,n-1}; \theta)$ and measurement density $f_{Y_{u,n}|X_{u,n}}(y_{u,n} | x_{u,n}; \theta)$ are permitted to depend arbitrarily on u and n , allowing non-stationary models and the inclusion of covariate time series (illustrated in Section 5). The framework also includes continuous-time dynamic models (illustrated in Section 6) and discrete-time dynamic models (illustrated in Sections 4.4 and 5), for which $X_{u,0:N_u}$ is specified directly without ever defining $\{X_u(t), t_{u,0} \leq t \leq t_{u,N_u}\}$.

The marginal density of $Y_{u,1:N_u}$ at $y_{u,1:N_u}$ is $f_{Y_{u,1:N_u}}(y_{u,1:N_u}; \theta)$ and the likelihood function for unit u is $\ell_u(\theta) = f_{Y_{u,1:N_u}}(y_{u,1:N_u}^*; \theta)$. The likelihood for the entire panel is $\ell(\theta) = \prod_{u=1}^U \ell_u(\theta)$, and any solution $\hat{\theta} = \arg \max \ell(\theta)$ is a maximum likelihood estimate (MLE).

Algorithm PIF. Panel iterated filtering

input:

Simulator of initial density, $f_{X_{u,0}}(x_{u,0}; \theta)$ for u in $1:U$

Simulator of transition density, $f_{X_{u,n}|X_{u,n-1}}(x_{u,n} | x_{u,n-1}; \theta)$ for u in $1:U$, n in $1:N_u$

Evaluator of measurement density, $f_{Y_{u,n}|X_{u,n}}(y_{u,n} | x_{u,n}; \theta)$ for u in $1:U$, n in $1:N_u$

Data, $y_{u,n}^*$ for u in $1:U$ and n in $1:N_u$

Number of iterations, M

Number of particles, J

Starting parameter swarm, Θ_j^0 for j in $1:J$

Simulator of perturbation density, $h_{u,n}(\theta | \varphi; \sigma)$ for u in $1:U$, n in $0:N_u$

Perturbation sequence, σ_m for m in $1:M$

output:

Final parameter swarm, Θ_j^M for j in $1:J$

For m in $1:M$

Set $\Theta_{0,j}^m = \Theta_j^{m-1}$ for j in $1:J$

For u in $1:U$

Set $\Theta_{u,0,j}^{F,m} \sim h_{u,0}(\theta | \Theta_{u-1,j}^m; \sigma_m)$ for j in $1:J$

Set $X_{u,0,j}^{F,m} \sim f_{X_{u,0}}(x_{u,0}; \Theta_{u,0,j}^{F,m})$ for j in $1:J$

For n in $1:N_u$

$\Theta_{u,n,j}^{P,m} \sim h_{u,n}(\theta | \Theta_{u,n-1,j}^{F,m}; \sigma_m)$ for j in $1:J$

$X_{u,n,j}^{P,m} \sim f_{X_{u,n}|X_{u,n-1}}(x_{u,n} | X_{u,n-1,j}^{F,m}; \Theta_{u,n,j}^{P,m})$ for j in $1:J$

$w_{u,n,j}^m = f_{Y_{u,n}|X_{u,n}}(y_{u,n}^* | X_{u,n,j}^{P,m}; \Theta_{u,n,j}^{P,m})$ for j in $1:J$

Draw $k_{1:J}$ with $\mathbb{P}(k_j = i) = w_{u,n,i}^m / \sum_{v=1}^J w_{u,n,v}^m$ for i, j in $1:J$

$\Theta_{u,n,j}^{F,m} = \Theta_{u,n,k_j}^{P,m}$ and $X_{u,n,j}^{F,m} = X_{u,n,k_j}^{P,m}$ for j in $1:J$

End For

Set $\Theta_{u,j}^m = \Theta_{u,N_u,j}^{F,m}$ for j in $1:J$

End For

Set $\Theta_j^m = \Theta_{U,j}^m$ for j in $1:J$

End For

The PIF algorithm, represented by the pseudocode above, is an adaptation of the IF2 algorithm (Ionides et al., 2015) to PanelPOMP models. The number of computations required for PIF has order $\mathcal{O}(JMNU)$, where N is the mean of $\{N_1, \dots, N_U\}$. The pseudocode specifies unique labels for each quantity constructed to clarify the logical structure of the algorithm, and a literal implementation of this pseudocode therefore requires storing $\mathcal{O}(JMNU)$ particles. Each particle contains a perturbed parameter vector and so has size $\mathcal{O}(U)$ if $\dim(\Theta)$ is $\mathcal{O}(U)$, leading to a total storage requirement of $\mathcal{O}(JMNU^2)$. However, we only need to store the value of the latent process particles, $X_{u,n,1:J}^{P,m}$ and $X_{u,n,1:J}^{F,m}$, and perturbed parameter particles, $\Theta_{u,n,1:J}^{P,m}$ and $\Theta_{u,n,1:J}^{F,m}$, for the current unit, time point and PIF iteration. Taking advantage of this memory over-writing opportunity leads to a storage requirement that is $\mathcal{O}(JU)$.

The theoretical justification of PIF is based on the observation that a PanelPOMP model can be represented as a time-inhomogeneous POMP model. Algorithms for PanelPOMPs, and their theoretical support, can therefore be derived from previous approaches for POMP. The supplement (Section S1) discusses the three different POMP representations of a PanelPOMP model noted by Romero-Severson et al. (2015). Here, we focus on a representation concatenating the time series for each unit, corresponding to a latent POMP process

$$X(t) = X_u \left(t_{u,0} + (t - T_{u-1}^{\text{cum}}) \right) \text{ for } T_{u-1}^{\text{cum}} \leq t \leq T_u^{\text{cum}} - 1, \quad (1)$$

where T_u^{cum} is a cumulative latent POMP process time for all panel units up to unit u , given by

$$T_u^{\text{cum}} = u + \sum_{k=1}^u (t_{k,N_k} - t_{k,0}) \quad (2)$$

and $T_0^{\text{cum}} = 0$. We leave $X(t)$ undefined for $T_{u-1}^{\text{cum}} - 1 < t < T_u^{\text{cum}}$ to provide a formal separation between the latent processes for each unit. In (2) we have set the value of this time separation to one, though any positive number would suffice and the exact value is irrelevant on the discrete timescale consisting of the sequence of observation times. This POMP representation is suitable for sequential Monte Carlo (SMC) based methodology since SMC has favorable stability properties for long time series under general conditions (Whiteley, 2013). We use this representation as a theoretical construct for motivating our PIF methodology; this does not imply actually concatenating the data for practical data analysis purposes.

3 Convergence of PIF

PIF investigates the parameter space using a particle swarm $\Theta_{1:J}^m = \{\Theta_j^m, j \in 1:J\}$. With a sufficiently large number J of particles, each iteration m of PIF approximates a Bayes map that selects a particle j with probability proportional to the value of the likelihood function at Θ_j^m . Heuristically, repeated application of the Bayes map favors particles with high likelihood and should lead to convergence of the particle swarm to a neighborhood of

the MLE. We state such a convergence theorem, followed by the technical assumptions we use to prove it.

Our theorem combines Theorems 1 and 2 of Ionides et al. (2015) in the context of the POMP representation of a PanelPOMP model in (1). Their Theorem 1 established conditions guaranteeing convergence of an iterated perturbed Bayes map to a probability density and its uniform approximation by SMC. Their Theorem 2 derived sufficient conditions for this density to concentrate around the MLE. Here, we combine these two theorems into a simpler statement.

Theorem 1. *Let $\Theta_{1:J}^M$ be the output of PIF, with fixed perturbations $\sigma_m = \delta$. Suppose regularity conditions A1–A6 below. For all $\epsilon > 0$, there exists δ , M_0 and C such that, for all $M \geq M_0$ and all $j \in 1:J$,*

$$\mathbb{P}\left[|\Theta_j^M - \hat{\theta}| > \epsilon\right] < \epsilon + \frac{C}{\sqrt{J}}. \quad (3)$$

To discuss the regularity conditions, we need to set up some more notation. We write $Y = (Y_{1,1:N_1}, \dots, Y_{U,1:N_U})$ and consequently we write y^* for a vector of the entire panel dataset. The likelihood function is $\ell(\theta) = f_Y(y^*; \theta)$ and we suppose the following regularity condition:

(A1) There is a unique MLE, and $\ell(\theta)$ is continuous in a neighborhood of this MLE.

To allow us to talk about parameter perturbations, we define a perturbed parameter space,

$$\check{\Theta} = \Theta^{N_1+1} \times \Theta^{N_2+1} \times \dots \times \Theta^{N_U+1},$$

for which we write $\check{\theta} \in \check{\Theta}$ as

$$\check{\theta} = (\theta_{1,0}, \theta_{1,1}, \dots, \theta_{1,N_1}, \theta_{2,0}, \dots, \theta_{2,N_2}, \dots, \theta_{U,N_U}). \quad (4)$$

For compatibility with the POMP representation of a PanelPOMP in (1), perturbed parameters for each time point and each unit are concatenated in (4) with $\theta_{u,n}$ being a perturbed parameter for the n th observation on unit u . On the perturbed parameter space $\check{\Theta}$, the extended likelihood function is defined as

$$\check{\ell}(\check{\theta}) = \prod_{u=1}^{N_U} \int \dots \int dx_{u,0} \dots dx_{u,N_U} \left\{ f_{X_{u,0}}(x_{u,0}; \check{\theta}_{u,0}) \prod_{n=1}^{N_u} f_{X_{u,n}|X_{u,n-1}}(x_{u,n} | x_{u,n-1}; \check{\theta}_{u,n}) f_{Y_{u,n}|X_{u,n}}(y_{u,n}^* | x_{u,n}; \check{\theta}_{u,n}) \right\}. \quad (5)$$

We suppose that the extended likelihood has a Lipschitz continuity property:

(A2) Set $\check{N} = \sum_{u=1}^U (N_u + 1)$, so that $\check{\Theta} = \Theta^{\check{N}}$. Write $\check{\theta}_n$ for the n th of the \check{N} terms in (4), so that $\check{\theta} = \theta_{1:\check{N}}$. There is a C_1 such that

$$|\check{\ell}(\check{\theta}) - \ell(\theta_{1,0})| < C_1 \sum_{n=2}^{\check{N}} |\check{\theta}_n - \check{\theta}_{n-1}|. \quad (6)$$

We also assume a uniformly positive measurement density:

(A3) There are constants C_2 and C_3 such that

$$0 < C_2 < f_{Y_{u,n}|X_{u,n}}(y_{u,n}^* | x_{u,n}; \theta) < C_3 < \infty,$$

for all $u \in 1:U$, $n \in 1:N_u$, $x_{u,n} \in \mathbb{X}_u$ and $\theta \in \Theta$.

This condition will usually require Θ and \mathbb{X}_u to be compact, for all $u \in 1:U$. Compactness of Θ is satisfied if there is some limit to the scientifically plausible values of each parameter. Compactness of \mathbb{X}_u may not be satisfied in practice, but much previous theory for SMC has used this strong requirement (e.g., Del Moral and Guionnet, 2001; Le Gland and Oudjane, 2004). The remaining conditions concern the perturbation transition density, $h_{u,n}(\theta | \varphi; \sigma)$. We suppose that $h_{u,n}(\theta | \varphi; \sigma)$ has bounded support on a normalized scale via the following condition:

(A4) There is a C_4 such that $h_{u,n}(\theta | \varphi; \sigma) = 0$ when $|\theta - \varphi| < C_4\sigma$ for all $u \in 1:U$, $n \in 1:N_u$ and σ .

We also require some regularity of an appropriately rescaled limit of the Markov chain resulting from iterating the perturbation process. Define $\{\check{\Theta}_m, m \geq 0\}$ to be a Markov chain taking values in Θ with $\check{\Theta}_0$ drawn uniformly from the starting particles, $\Theta_{1:J}^0$, and transition density given by

$$f_{\check{\Theta}_m|\check{\Theta}_{m-1}}(\theta_{U,N_U} | \varphi; \sigma) = \int \left\{ h_{1,0}(\theta_{1,0} | \varphi; \sigma) \prod_{u=2}^U h_{u,0}(\theta_{u,0} | \theta_{u-1,N_{u-1}}; \sigma) d\theta_{u-1,N_{u-1}} \prod_{u=1}^U \prod_{n=1}^{N_u} h_{u,n}(\theta_{u,n} | \theta_{u,n-1}; \sigma) d\theta_{u,n-1} \right\}. \quad (7)$$

Thus, $\{\check{\Theta}_m\}$ represents a random-walk-like process corresponding to combining the parameter perturbations of all units and all time points for one iteration of PIF. Now, let $\{W_\sigma(t), t \geq 0\}$ be a right-continuous, piecewise constant process taking values in Θ defined at its points of discontinuity by

$$W_\sigma(k\sigma^2) = \check{\Theta}_k. \quad (8)$$

If $h_{u,n}(\theta | \varphi; \sigma)$ were a scale family of additive perturbations, then $\{\check{\Theta}_m\}$ would be a random walk that scales to a Brownian diffusion. When Θ has a boundary, $\{\check{\Theta}_m\}$ cannot be exactly a random walk, but similar diffusion limits can apply (Bossy et al., 2004). We require that $h_{u,n}(\theta | \varphi; \sigma)$ is chosen to be sufficiently regular to have such a diffusion limit, via the following assumptions:

(A5) $\{W_\sigma(t), 0 \leq t \leq 1\}$ converges weakly as $\sigma \rightarrow 0$ to a diffusion $\{W(t), 0 \leq t \leq 1\}$, in the space of right-continuous functions with left limits equipped with the uniform convergence topology. For any open set $A \subset \Theta$ with positive Lebesgue measure and $\epsilon > 0$, there is a $\delta(A, \epsilon) > 0$ such that $\mathbb{P}[W(t) \in A \text{ for all } \epsilon \leq t \leq 1 | W(0)] > \delta$.

(A6) For some $t_0(\sigma)$ and $\sigma_0 > 0$, $W_\sigma(t)$ has a positive density on Θ , uniformly over the distribution of $W(0)$ for all $t > t_0$ and $\sigma < \sigma_0$.

Proof of Theorem 1. PIF is exactly the IF2 algorithm of Ionides et al. (2015) applied to the POMP representation of a PanelPOMP model in equation (1). A1 is condition B3 of Ionides et al. (2015) together with a simplifying additional assumption that a unique MLE exists. A2 is a re-writing of their B6. A3 and A4 are essentially their B4 and B5. A5 and A6 match their B1 and B2, respectively. Thus, we have established the conditions used for Theorems 1 and 2 of Ionides et al. (2015) for this POMP representation of a PanelPOMP model. The statement of our Theorem 1 follows directly from these two previous results. \square

The perturbation density $h_{u,n}(\theta|\varphi;\sigma)$ has usually been chosen to be Gaussian in implementations of the IF2 algorithm and its predecessor, the IF1 algorithm (Ionides et al., 2006). The use of Gaussian perturbations requires the user to reparameterize boundaries in the parameter space. It also does not formally satisfy assumption A4, though the Gaussian distribution has short tails that are heuristically compatible with this assumption. Gaussian perturbations permit an alternative theoretical framework for approximating derivatives via SMC using Stein’s lemma (Doucet, Jacob and Rubenthaler, 2015; Dai and Schön, 2016). The resulting derivatives underly the theoretical justification provided by Ionides et al. (2006) for the IF1 algorithm. The iterated perturbed Bayes map underlying the IF2 algorithm can lead to greater numerical stability and better performance on challenging problems than IF1, as reported by Ionides et al. (2015).

4 Scalable methodology for large panels

Theorem 1 provides an asymptotic Monte Carlo convergence guarantee for a dataset of fixed size as the Monte Carlo effort increases. In practice, reaching this asymptotic regime becomes increasingly difficult as the panel dataset grows, whether the number of units becomes large, or there are many observations per unit, or both. In this section, we consider some techniques that become important when using PIF for big datasets. We demonstrate the methodology on a toy model in Section 4.4. Subsequently, we demonstrate data analysis for mechanistic panel models using PIF via two examples, one investigating disease transmission of polio and another investigating dynamics of human sexual behavior.

4.1 Monte Carlo adjusted profile (MCAP) confidence intervals

PIF provides a Monte Carlo approach to maximizing the likelihood function for a PanelPOMP model. It is based on an SMC algorithm that can also provide an unbiased estimate of the maximized likelihood. Monte Carlo methods to evaluate and maximize the likelihood function provide a foundation for constructing confidence intervals via profile likelihood. When computational resources are sufficient to make Monte Carlo error small, its role in statistical inference may be negligible. With large datasets and complex models, we cannot ignore Monte Carlo error so instead we quantify it and draw statistical inferences that properly account for it. We use the Monte Carlo adjusted profile (MCAP) methodology of Ionides et al. (2017) which fits a smooth curve through Monte Carlo evaluations of points

on a profile log likelihood. MCAP then obtains a confidence interval using a cutoff on this estimated profile that is enlarged to give proper coverage despite Monte Carlo uncertainty in its construction. Monte Carlo variability in maximizing and evaluating the likelihood both lead to expected under-estimation of the maximized log likelihood. Despite such bias the MCAP methodology remains valid as long as this *likelihood shortfall* is slowly varying as a function of the profiled parameter. Our toy example in Section 4.4 demonstrates this phenomenon. The MCAP procedure is used for all our subsequent examples.

4.2 Marginal maximization for unit-specific parameters

The parameter space for a PanelPOMP model may be structured into unit-specific and shared parameters. To do this, we introduce a decomposition $\Theta = \Phi \times \Psi^U$ and $\theta = (\phi, \psi_1, \psi_2, \dots, \psi_U)$ with the joint distribution of $X_{u,0:N_u}$ and $Y_{u,1:N_u}$, for each unit u , depending only on the shared parameter $\phi \in \Phi \subset \mathbb{R}^{\dim(\Phi)}$ and the unit-specific parameter $\psi_u \in \Psi \subset \mathbb{R}^{\dim(\Psi)}$. The general PanelPOMP specification does not insist on the existence of unit-specific parameters but, when they exist, the additional structure can be used to advantage.

When U is large, $\dim(\Theta) = \dim(\Phi) + U\dim(\Psi)$ also becomes large. For a fixed value of ϕ , the marginal likelihoods of $\psi_{1:U}$ can be maximized separately, due to independence between units. Formally, application of iterated filtering to each of these marginal optimizations is a special case of the PIF algorithm with $U = 1$. Thus, the convergence theory for PIF gives us freedom to alternate marginal optimization steps with joint optimization over Θ , following a block coordinate ascent approach. In practice, we demonstrate a simple two-step algorithm which first attempts to optimize over Θ and then refines the resulting estimates of the unit-specific parameters by marginal searches for each unit. Figure 1 of Section 4.4 shows that this leads to considerable Monte Carlo variance reduction on an analytically tractable example.

4.3 Using replications for likelihood maximization and evaluation

Monte Carlo replication, with differing random number generator seed values, is a basic tool for obtaining and assessing Monte Carlo approximations to a maximum likelihood estimate and its corresponding maximized likelihood. Replication is trivially parallelizable, so provides a simple strategy to take advantage of large numbers of computer processors. Repeated searches, from wide-ranging starting values, provide a practical assessment of the success of global maximization. When many Monte Carlo searches have found a comparable maximized likelihood, and no searches have surpassed it, we have some confidence that the likelihood surface has been adequately investigated.

PIF requires an additional calculation to evaluate the likelihood at the proposed maximum. The PIF algorithm produces an estimate of the likelihood for the perturbed model, and if the perturbations are small this may provide a useful approximation to the likelihood, however re-evaluation with the unperturbed model is appropriate for likelihood-based inference. Making R replicated Monte Carlo evaluations of the likelihood gives rise to estimates $\{\ell_u^{(r)}, r \in 1:R, u \in 1:U\}$ for each replication and unit. One possible way to combine these

is an estimate $\tilde{\ell} = \frac{1}{R} \sum_{r=1}^R \prod_{u=1}^U \ell_u^{(r)}$. When computed via SMC, this estimate is unbiased (Theorem 7.4.2 on page 239 in Del Moral, 2004). However, we use an alternative unbiased estimate, $\hat{\ell} = \prod_{u=1}^U \frac{1}{R} \sum_{r=1}^R \ell_u^{(r)}$, which has lower variance (derived in Section S2).

4.4 A toy example: the panel Gompertz model

We consider a PanelPOMP constructed as a stochastic version of the discrete-time Gompertz model for biological population growth (Winsor, 1932). We suppose that the density, $X_{u,n+1}$, of a population u at time $n + 1$ depends on the density, $X_{u,n}$, at time n according to

$$X_{u,n+1} = \kappa_u^{1-e^{-r_u}} X_{u,n}^{e^{-r_u}} \varepsilon_{u,n}. \quad (9)$$

In (9), κ_u is the carrying capacity of population u , r_u is a positive parameter, and $\{\varepsilon_{u,n}, u \in 1:U, n \in 1:N_u\}$ are independent and identically-distributed lognormal random variables with $\log \varepsilon_{u,n} \sim \text{Normal}(0, \sigma_{G,u}^2)$. We model the population density to be observed with errors in measurement that are lognormally distributed:

$$\log Y_{u,n} \sim \text{Normal}(\log X_{u,n}, \tau_u^2).$$

The Gompertz model is a convenient toy nonlinear non-Gaussian model since it has a logarithmic transformation to a linear Gaussian process and therefore the exact likelihood is computable by the Kalman filter (King et al., 2016). As discussed in Section 4.1, we expect Monte Carlo estimates of profile log likelihood functions to fall below the actual (usually unknown) value. This is in part because imperfect maximization can only reduce the maximized likelihood, and in part a consequence of Jensen’s inequality applied to the likelihood evaluation: the unbiased SMC likelihood evaluation has a negative bias on estimation of the log likelihood. However, this bias produces a vertical shift in the estimated profile that may (and, in this example, does) have negligible effect on the resulting confidence interval.

For our experiment, we used $N_u = 100$ simulated observations for each of $U = 50$ panel units. For each $u \in 1:U$, we fixed $\kappa_u = 1$ and $X_{u,0} = 1$. We set $\sigma_{G,u} = \sigma_G = 0.1$ and $r_u = r = 0.1$. We estimated the shared parameters σ_G and r . We also estimated unit-specific parameters $\tau_{1:U}$ with true values set to $\tau_u = 0.1$. We profiled over the shared parameter σ_G , maximizing with respect to r and the 50 unit-specific parameters $\tau_{1:U}$. In Figure 1, the estimated profile using the marginal step has a log likelihood shortfall of only approximately $3.4/51 = 0.07$ log units per parameter. By contrast, maximization using only the joint step has a shortfall of $28.1/51 = 0.6$ per parameter and substantially greater Monte Carlo variability. This greater variability leads to a larger Monte Carlo adjusted profile cut-off than the asymptotic value of 1.92, and therefore typically produces a wider 95% confidence interval (Ionides et al., 2017).

5 Polio: state-level pre-vaccination incidence in USA

The study of ecological and epidemiological systems poses challenges involving nonlinear mechanistic modeling of partially observed processes (Bjørnstad and Grenfell, 2001). Here,

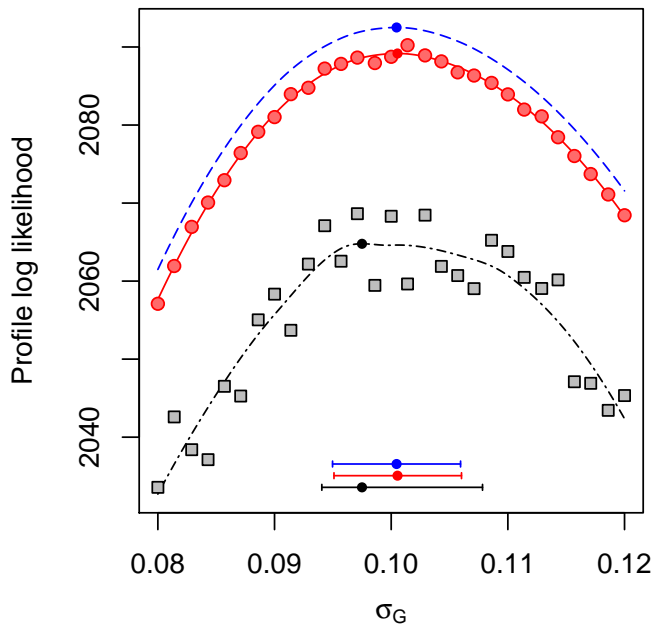


Figure 1: Profile log likelihood of σ_G for a panel of size $U = 50$ for the Gompertz model. Blue line (dashes): exact profile. Red points and line (circles): profile computed with PIF, including marginal maximization for unit-specific parameters. Black points and line (squares): profile computed with PIF using only joint maximization. The horizontal bars show 95% MCAP confidence intervals with a small filled circle marking the MLE obtained with algorithmic parameters in table S-1 in the supplement.

we illustrate this class of models and data, in the context of panel data analysis, by analyzing state-level historic polio incidence data in USA. Although introduction of a pathogen into a host community requires contact between communities, the vast majority of infectious disease transmission events have infector and infectee within the same community (Bjørnstad et al., 2002). Therefore, for the purpose of understanding the dynamics of infectious diseases within communities, one may choose to model a collection of communities as independent conditional on a pathogen immigration process. For example, fitting a panel model to epidemic data on a collection of geographical regions could permit statistical identification of dynamic mechanisms that cannot readily be detected by the data available in any one region. Further, differences between regions (in terms of size, climate, and other demographic or geographic factors) may lead to varying disease dynamics that can challenge and inform a panel model.

The massive efforts of the global polio eradication initiative have brought polio from a major global disease to the brink of extinction (Patel and Orenstein, 2016). Finishing this task is proving hard, and an improved understanding of polio ecology might assist. Martinez-Bakker et al. (2015) investigated polio dynamics by fitting a mechanistic model to pre-vaccination era data from the USA consisting of monthly reports of acute paralysis from May 1932 through January 1953. Reports are available for the 48 contiguous US states and

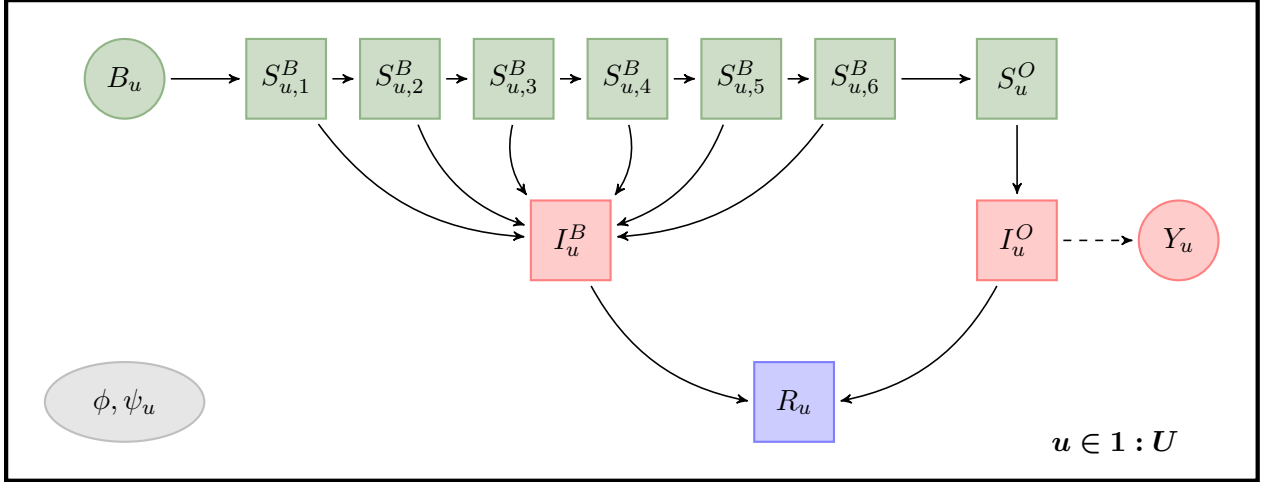


Figure 2: Flow diagram for the polio panel model. Each individual resides in exactly one of the compartments denoted by square boxes. Solid arrows represent possible transitions into a new compartment. Circles represent observed variables: the reported incidence, Y_u , and births, B_u . The dependence of Y_u on I_u^O is denoted by a dashed arrow. Colors and rows represent disease status: unexposed is green (top row); infected is red (middle row); recovered is purple (bottom row). The panel structure is indicated by the replication of this model over $u \in 1:U$. The shared parameter vector $\phi = (\rho, \sigma_{\text{dem}}, \psi, \tau)$ and unit-specific parameter $\psi_u = (b_{u,1:6}, \sigma_{\text{env},u}, \tilde{S}_{u,0}^O, \tilde{I}_{u,0}^O)$ are identified in the gray ellipse.

Washington D.C., so $U = 49$, and henceforth we refer to these units as states. A sample of the time series in this panel is plotted in the supplement. Martinez-Bakker et al. (2015) fitted their model separately to each state which, in panel terminology, amounted to a decision to make all parameters unit-specific. Some parameters, such as duration of infection, might be well modeled as shared between all units. Other parameters, such as the model for seasonality of disease transmission, should intuitively be slowly varying geographically. Martinez-Bakker et al. (2015) did not have access to panel inference methodology, and so here we reconsider their model and data and investigate what happens when some parameters become shared between units.

The model of Martinez-Bakker et al. (2015) places each individual in the population into one of ten compartments: susceptible babies in each of six one-month birth cohorts (S_1^B, \dots, S_6^B), susceptible older individuals (S^O), infected babies (I^B), infected older individuals (I^O), and individuals who have recovered with lifelong immunity (R). Our PanelPOMP version of their model has a latent process determining the number of individuals in each compartment at each time for each unit $u \in 1:U$. We write

$$X_u(t) = (S_{u,1}^B(t), \dots, S_{u,6}^B(t), I_u^B(t), S_u^O(t), I_u^O(t), R_u(t)).$$

The flows through the compartments are graphically represented in Figure 2. Births for each state u are treated as a covariate time series, known from census data (Martinez-Bakker et al., 2014). Babies under six months are modeled as fully protected from paralytic

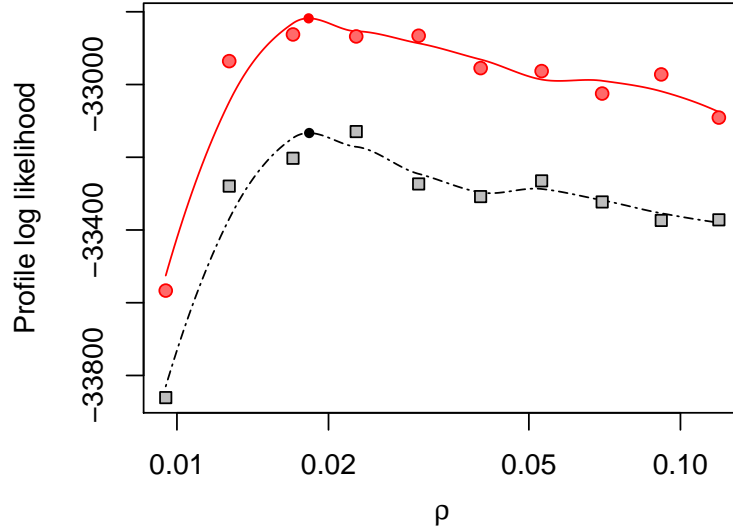


Figure 3: Profile log likelihood of ρ for the polio model, computed with marginal maximization for unit-specific parameters (red circles and line) and without (black squares and line) with algorithmic parameters in table S-1 in the supplement. Figure 4 gives a closer look in a neighborhood of the maximum and constructs a confidence interval.

polio, but capable of a gastro-intestinal polio infection. Infection of an older individual leads to a reported paralytic polio case with probability ρ_u .

Since duration of infection is comparable to the one-month reporting aggregation, a discrete time model may be appropriate. The model is therefore specified only at times $t_{u,n} = t_n = 1932 + (4 + n)/12$ for $n = 0, \dots, 249$. We write

$$X_{u,n} = X_u(t_n) = (S_{u,1,n}^B, \dots, S_{u,6,n}^B, S_{u,n}^O, I_{u,n}^B, I_{u,n}^O, R_{u,n}).$$

The mean force of infection, in units of yr^{-1} , is modeled as

$$\bar{\lambda}_{u,n} = \left(\beta_{u,n} \frac{I_{u,n}^O + I_{u,n}^B}{P_{u,n}} + \psi \right),$$

where $P_{u,n}$ is a census population covariate for state u interpolated to time t_n and seasonality of transmission is modeled as

$$\beta_{u,n} = \exp \left\{ \sum_{k=1}^K b_{u,k} \xi_k(t_n) \right\},$$

with $\{\xi_k(t), k = 1, \dots, K\}$ being a periodic B-spline basis. We set $K = 6$. The force of infection has a stochastic perturbation,

$$\lambda_{u,n} = \bar{\lambda}_{u,n} \epsilon_{u,n},$$

where $\epsilon_{u,n}$ is a Gamma random variable with mean 1 and variance $\sigma_{\text{env},u}^2 + \sigma_{\text{dem},u}^2 [\lambda_{u,n}]^{-1}$. These two terms capture variation on the environmental and demographic scales, respectively

(Bretó et al., 2009). All compartments suffer a mortality rate, set at $\delta = [60 \text{ yr}]^{-1}$ for all states. Within each month, all susceptible individuals are modeled as having exposure to constant competing hazards of mortality and polio infection. The chance of remaining in the susceptible population when exposed to these hazards for one month is therefore

$$p_{u,n} = \exp \left\{ -\frac{\delta + \lambda_{u,n}}{12} \right\},$$

with the chance of polio infection being

$$q_{u,n} = (1 - p_{u,n}) \frac{\lambda_{u,n}}{\lambda_{u,n} + \delta}.$$

We employ a continuous population model: writing $B_{u,n}$ for births in month n for state u , the full set of model equations is,

$$\begin{aligned} I_{u,n+1}^B &= q_{u,n} \sum_{k=1}^6 S_{u,k,n}^B, & S_{u,1,n+1}^B &= B_{u,n+1}, & S_{u,k,n+1}^B &= p_{u,n} S_{u,k-1,n}^B \text{ for } k \in 1:6, \\ I_{u,n+1}^O &= q_{u,n} S_{u,n}^O, & S_{u,n+1}^O &= p_{u,n} (S_{u,n}^O + S_{u,6,n}^B). \end{aligned}$$

The model for the reported observations, conditional on the latent process, is a discretized normal distribution truncated at zero, with both environmental and Poisson-scale contributions to the variance:

$$Y_{u,n} = \max\{\text{round}(Z_{u,n}), 0\}, \quad Z_{u,n} \sim \text{Normal} \left(\rho I_{u,n}^O, \rho_u I_{u,n}^O + (\tau_u I_{u,n}^O)^2 \right),$$

where $\text{round}(x)$ obtains the integer closest to x . Additional parameters are used to specify initial values for the latent process at time $t_0 = 1932 + 4/12$. We will suppose there are parameters $(\tilde{S}_{u,1,0}^B, \dots, \tilde{S}_{u,6,0}^B, \tilde{I}_{u,0}^B, \tilde{I}_{u,0}^O, \tilde{S}_{u,0}^O)$ that specify the population in each compartment at time t_0 via

$$S_{u,1,0}^B = \tilde{S}_{u,1,0}^B, \dots, S_{u,6,0}^B = \tilde{S}_{u,6,0}^B, \quad I_{u,0}^B = P_{u,0} \tilde{I}_{u,0}^B, \quad S_{u,0}^O = P_{u,0} \tilde{S}_{u,0}^O, \quad I_{u,0}^O = P_{u,0} \tilde{I}_{u,0}^O.$$

The initial conditions are simplified by ignoring infant infections at time t_0 . Thus, we set $\tilde{I}_{u,0}^B = 0$ and use monthly births in the preceding months (ignoring infant mortality) to fix $\tilde{S}_{u,k,0}^B = B_{u,1-k}$ for $k = 1, \dots, 6$. The estimated initial conditions for state u are then defined by the two parameters $\tilde{I}_{u,0}^O$ and $\tilde{S}_{u,0}^O$, since the initial recovered population, $R_{u,0}$, is specified by subtraction of all the other compartments from the total initial population, $P_{u,0}$.

Figure 3 shows the profile likelihood for the shared reporting rate, ρ , evaluated across a wide interval to investigate large-scale features of the likelihood surface. Including a marginal maximization step in PIF leads to gains in agreement with the findings of Figure 1. Figure 3 indicates an MLE around 0.02 and so this parameter range was studied further in a higher resolution profile in Figure 4. On this localized plot, we can see Monte Carlo error of order 10 log units in the maximization and evaluation of the log likelihood. Since construction

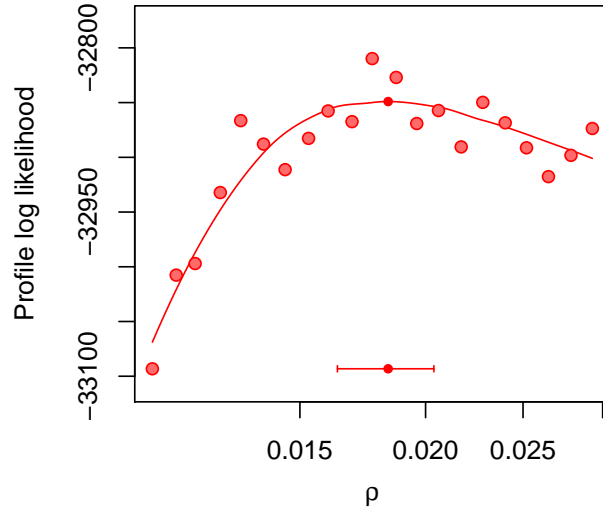


Figure 4: Profile log likelihood of ρ for the polio model, computed in a neighborhood of the MLE. The horizontal bar shows a 95% MCAP confidence interval with a small filled circle marking the MLE obtained with algorithmic parameters in table S-1 in the supplement.

of this plot employed 528.0 core days of computational effort, we had limited capacity for further reductions in Monte Carlo error by further increases in computation. Fortunately, MCAP methodology is able to handle Monte Carlo error on this scale: see, for example, the noisiest profile in Figure 1 using only joint maximization. The resulting 95% confidence interval from Figure 4 is (0.016, 0.020), which is consistent with estimates for the fraction of polio infections leading to acute paralysis in USA in this era (Melnick and Ledinko, 1953). By contrast, Martinez-Bakker et al. (2015) found point estimates ranging from 0.0025 to 0.03 when analyzing each state separately, with wide confidence intervals evident from the profiles in their Figures S9–S17.

6 Dynamic variation in sexual contact rates

We demonstrate PIF for analysis of panel data on sexual contacts, using the model and data of Romero-Severson et al. (2015). The data consist of many short time series, a common situation in classical longitudinal analysis. We show that PIF provides useful flexibility to permit consideration of scientifically relevant dynamic models including latent dynamic variables.

Basic population-level disease transmission models suppose equal contact rates for all individuals in a population (Keeling and Rohani, 2008). Sometimes these models are extended to permit heterogeneity between individuals. Heterogeneity within individuals over time has rarely been considered, yet, there have been some indications that dynamic behavioral change plays a substantial role in the HIV epidemic. Romero-Severson et al. (2015) quantified dynamic changes in sexual behavior by fitting a model for dynamic variation in sexual contact rates to panel data from a large cohort study of HIV-negative gay men (Vittinghoff

et al., 1999). Here, we analyze the data on total sexual contacts over $N_u = 4$ consecutive 6-month periods for the $U = 882$ men in the study who had no missing observations. A sample of the time series in this panel is plotted in the supplement.

For behavioral studies, we interpret “mechanistic model” broadly to mean a mathematical model describing phenomena of interest via interpretable parameters. In this context, we want a model that can describe (i) differences between individuals; (ii) differences within individuals over time; (iii) flexible relationships between mean and variance of contact rates. Romero-Severson et al. (2015) developed a PanelPOMP model capturing these phenomena. Suppose that each individual $u \in 1:U$ has a latent time-varying rate $\Lambda_u(t)$ of making a sexual contact. Each data point, $y_{u,n}^*$, is the number of reported contacts for individual u between time $t_{u,n-1}$ and $t_{u,n}$. Integrating the unobserved process $\{\Lambda_u(t)\}$ gives the conditional expected value in (10) of contacts for individual u in reporting interval n , via

$$C_{u,n} = \alpha^{n-1} \int_{t_{u,n-1}}^{t_{u,n}} \Lambda_u(t) dt,$$

where α is an additional secular trend that accounts for the observed decline in reported contacts. A basic stochastic model for homogeneous count data would model $y_{u,n}^*$ as a Poisson random variable with mean and variance equal to $C_{u,n}$ (Keeling and Rohani, 2008). However, the variance in the data is much higher than the mean (Romero-Severson et al., 2012). Negative binomial processes provide a route to modeling dynamic over-dispersion (Bretó and Ionides, 2011). Here, we suppose that

$$Y_{u,n} | C_{u,n}, D_u \sim \text{NegBin}(C_{u,n}, D_u), \quad (10)$$

a conditional negative binomial distribution with mean $C_{u,n}$ and variance $C_{u,n} + C_{u,n}^2 [D_u]^{-1}$. Here, D_u is called the dispersion parameter, with the Poisson model being recovered in the limit as D_u becomes large. The dispersion, D_u , can model increased variance compared to the Poisson distribution for individual contacts, but does not result in autocorrelation between measurements on an individual over time, which is observed in the data. To model this autocorrelation, we suppose that individual u has behavioral episodes of exponentially distributed duration within which $\{\Lambda_u(t)\}$ is constant, but the individual enters new behavioral episodes at rate μ_R . At the start of each episode, $\{\Lambda_u(t)\}$ takes a new value drawn from a Gamma distribution with mean μ_X and standard deviation σ_X . Therefore, at each time t ,

$$\Lambda_u(t) \sim \text{Gamma}(\mu_X, \sigma_X).$$

To complete the model, we also assume $D_u \sim \text{Gamma}(\mu_D, \sigma_D)$. The parameter vector is $\theta = (\mu_X, \sigma_X, \mu_D, \sigma_D, \mu_R, \alpha)$.

Figure 5 constructs a profile likelihood confidence interval for μ_R . This result is comparable to Web Figure 1 of Romero-Severson et al. (2015), however, here we have shown how this example fits into a general methodological framework. The profile demonstrates an intermediate level of computational challenge between the relatively simple Gompertz example of Section 4.4 and the extensive data, complex model, and correspondingly larger Monte

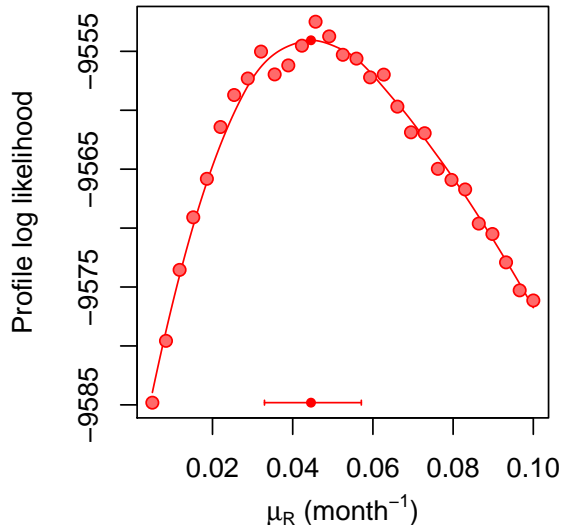


Figure 5: Profile log likelihood of μ_R for a panel of size $U = 882$ for the contacts model. The horizontal bar shows a 95% MCAP confidence interval with a small filled circle marking the MLE obtained with algorithmic parameters in table S-1 in the supplement.

Carlo computations of Section 5. Figure 5 took 68.7 core days to compute. No marginal maximization was necessary for this example, since all parameters were shared between all units.

7 Discussion

When panel data are short, relative to the complexity of the model under consideration, there may be little information in the data about each unit-specific parameter. In such cases, it can be appropriate to replace some unit-specific parameters by latent random variables. By analogy with linear regression analysis, these unit-specific latent random variables are called *random effects*, and unit-specific parameters treated as unknown constants are called *fixed effects*. Models with random effects are also called *hierarchical* models, since an additional hierarchy of modeling is required to describe the additional latent variables, and parameters of the random effect distribution are consequently termed *hyperparameters*. From the perspective of statistical inference, using random effects reduces the number of fitted parameters, at the expense of adding additional modeling assumptions. From the perspective of computation, random effects reduce the dimensionality of the likelihood optimization challenge, while increasing the dimensionality of the latent space which must be integrated over to evaluate the likelihood. The use of random effects provides an opportunity for the estimation of individual unit-specific effects to borrow strength from other panel units, via estimation of the hyperparameters. Therefore, random effects can have particular value if one is interested in estimating the unit-specific effects. However, when the research question is focused on shared parameters or higher-level model structure decisions such as whether a

parameter should be included in the model, the individual unit-specific parameters can be a distraction. Rather than spending time developing and justifying a distribution for the random effects, simpler statistical reasoning can be obtained by avoiding these issues and employing fixed effects.

The sexual contact model has random effects D_u and has no fixed effects. This is appropriate for panel data with very short time series. By contrast, the polio data are relatively long time series, favoring the use of fixed effects.

Panel time series analysis shares similarities with functional data analysis (Ramsay and Silverman, 1997). Within functional data analysis, a representation of dynamic mechanisms can be incorporated via principal differential analysis (Ramsay, 1996). Partially observed stochastic dynamic models are not within the usual scope of the field of functional data analysis, though there is no need for a hard line separating functional data analysis from panel data analysis.

We wrote an R package, `panelPomp`, that provides a software environment for developing methodology and data analysis tools for PanelPOMP models. This package is available at <https://github.com/cbreto/panelPomp>. The current version of `panelPomp` is focused on SMC methods, and in particular the PIF algorithm. The computational framework could also facilitate future implementation of other panel methods. In particular, `panelPomp` extends the `pomp` package (King et al., 2016) and so we anticipate that panel analogs of other POMP methods already implemented in `pomp` could be developed.

Iterated filtering algorithms provide an approach to full-information likelihood-based inference that is plug-and-play and that has been applied in challenging nonlinear mechanistic time series analyses, especially in epidemiology (reviewed by Bretó, 2017). Reduced information methods, such as those using simulations to compare the data with a collection of summary statistics, can lead to substantial losses in statistical efficiency (Fasiolo et al., 2016; Shrestha et al., 2011). Particle Markov chain Monte Carlo (Andrieu et al., 2010) provides a route to plug-and-play full-information Bayesian inference, but the methodology requires computational feasibility of log likelihood estimates with a standard error of around 1 log unit (Doucet, Pitt, Deligiannidis and Kohn, 2015). PIF is the first plug-and-play full-information likelihood-based approach demonstrated to be applicable on general partially observed nonlinear stochastic dynamic models for panel data analysis on the scale we have considered.

References

- Andrieu, C., Doucet, A. and Holenstein, R. (2010), ‘Particle Markov chain Monte Carlo methods’, *Journal of the Royal Statistical Society, Series B (Statistical Methodology)* **72**(3), 269–342.
- Bartolucci, F., Farcomeni, A. and Pennoni, F. (2012), *Latent Markov models for longitudinal data*, CRC Press.
- Bjørnstad, O. N., Finkenstädt, B. F. and Grenfell, B. T. (2002), ‘Dynamics of measles epi-

- demics: Estimating scaling of transmission rates using a time series SIR model’, *Ecological Monographs* **72**, 169–184.
- Bjørnstad, O. N. and Grenfell, B. T. (2001), ‘Noisy clockwork: Time series analysis of population fluctuations in animals’, *Science* **293**, 638–643.
- Bossy, M., Gobet, E. and Talay, D. (2004), ‘A symmetrized Euler scheme for an efficient approximation of reflected diffusions’, *Journal of Applied Probability* **41**(3), 877–889.
- Bretó, C. (2017), ‘Modeling and inference for infectious disease dynamics: a likelihood-based approach’, *Statistical Science*, pre-published online.
- Bretó, C., He, D., Ionides, E. L. and King, A. A. (2009), ‘Time series analysis via mechanistic models’, *Annals of Applied Statistics* **3**, 319–348.
- Bretó, C. and Ionides, E. L. (2011), ‘Compound Markov counting processes and their applications to modeling infinitesimally over-dispersed systems’, *Stochastic Processes and their Applications* **121**, 2571–2591.
- Cauchemez, S., Carrat, F., Viboud, C., Valleron, A. J. and Boelle, P. Y. (2004), ‘A Bayesian MCMC approach to study transmission of influenza: Application to household longitudinal data’, *Statistics in Medicine* **23**, 3469–3487.
- Chen, Y., Shen, K., Shan, S.-O. and Kou, S. (2016), ‘Analyzing single-molecule protein transportation experiments via hierarchical hidden Markov models’, *Journal of the American Statistical Association* **111**(515), 951–966.
- Dai, L. and Schön, T. B. (2016), ‘Using convolution to estimate the score function for intractable state-transition models’, *IEEE Signal Processing Letters* **23**(4), 498–501.
- Del Moral, P. (2004), *Feynman-Kac Formulae: Genealogical and Interacting Particle Systems with Applications*, Springer, New York.
- Del Moral, P. and Guionnet, A. (2001), ‘On the stability of interacting processes with applications to filtering and genetic algorithms’, *Annales de l’Institut Henri Poincaré (B) Probability and Statistics* **37**(2), 155–194.
- Dobson, A. (2014), ‘Mathematical models for emerging disease’, *Science* **346**(6215), 1294–1295.
- Donnet, S. and Samson, A. (2013), ‘A review on estimation of stochastic differential equations for pharmacokinetic/pharmacodynamic models’, *Advanced Drug Delivery Reviews* **65**(7), 929–939.
- Douc, R., Moulines, E. and Stoffer, D. (2014), *Nonlinear time series: Theory, methods and applications with R examples*, CRC Press.

- Doucet, A., Jacob, P. E. and Rubenthaler, S. (2015), ‘Derivative-free estimation of the score vector and observed information matrix with application to state-space models’, *arXiv:1304.5768v3*.
- Doucet, A., Pitt, M. K., Deligiannidis, G. and Kohn, R. (2015), ‘Efficient implementation of Markov chain Monte Carlo when using an unbiased likelihood estimator’, *Biometrika* **102**, 295–313.
- Fasiolo, M., Pya, N. and Wood, S. N. (2016), ‘A comparison of inferential methods for highly nonlinear state space models in ecology and epidemiology’, *Statistical Science* **31**(1), 96–118.
- He, D., Ionides, E. L. and King, A. A. (2010), ‘Plug-and-play inference for disease dynamics: Measles in large and small towns as a case study’, *Journal of the Royal Society Interface* **7**, 271–283.
- Heiss, F. (2008), ‘Sequential numerical integration in nonlinear state space models for microeconomic panel data’, *Journal of Applied Econometrics* **23**(3), 373–389.
- Hsiao, C. (2014), *Analysis of Panel Data*, Cambridge University Press, Cambridge, UK.
- Ionides, E. L., Bretó, C. and King, A. A. (2006), ‘Inference for nonlinear dynamical systems’, *Proceedings of the National Academy of Sciences of the USA* **103**, 18438–18443.
- Ionides, E. L., Breto, C., Park, J., Smith, R. A. and King, A. A. (2017), ‘Monte Carlo profile confidence intervals for dynamic systems’, *Journal of the Royal Society Interface* **14**, 1–10.
- Ionides, E. L., Nguyen, D., Atchadé, Y., Stoev, S. and King, A. A. (2015), ‘Inference for dynamic and latent variable models via iterated, perturbed Bayes maps’, *Proceedings of the National Academy of Sciences of the USA* **112**(3), 719–724.
- Keeling, M. J. and Rohani, P. (2008), *Modeling infectious diseases in humans and animals*, Princeton University Press.
- King, A. A., Nguyen, D. and Ionides, E. L. (2016), ‘Statistical inference for partially observed Markov processes via the R package pomp’, *Journal of Statistical Software* **69**, 1–43.
- Le Gland, F. and Oudjane, N. (2004), ‘Stability and uniform approximation of nonlinear filters using the Hilbert metric and application to particle filters’, *The Annals of Applied Probability* **14**(1), 144–187.
- Martinez-Bakker, M., Bakker, K. M., King, A. A. and Rohani, P. (2014), ‘Human birth seasonality: latitudinal gradient and interplay with childhood disease dynamics’, *Proceedings of the Royal Society of London B: Biological Sciences* **281**(1783).
- Martinez-Bakker, M., King, A. A. and Rohani, P. (2015), ‘Unraveling the transmission ecology of polio’, *PLoS Biology* **13**(6), e1002172.

- Melnick, J. L. and Ledinko, N. (1953), ‘Development of neutralizing antibodies against the three types of poliomyelitis virus during an epidemic period. the ratio of inapparent infection to clinical poliomyelitis’, *American Journal of Hygiene* **58**(2), 207–22.
- Mesters, G. and Koopman, S. J. (2014), ‘Generalized dynamic panel data models with random effects for cross-section and time’, *Journal of Econometrics* **180**, 127–140.
- Patel, M. and Orenstein, W. (2016), ‘A world free of polio – the final steps’, *New England Journal of Medicine* **374**(6), 501–503.
- Ramsay, J. O. (1996), ‘Principal differential analysis: Data reduction by differential operators’, *Journal of the Royal Statistical Society, Series B (Statistical Methodology)* **58**, 495–508.
- Ramsay, J. O. and Silverman, B. W. (1997), *Functional Data Analysis*, Springer-Verlag, New York.
- Romero-Severson, E. O., Alam, S. J., Volz, E. M. and Koopman, J. S. (2012), ‘Heterogeneity in number and type of sexual contacts in a gay urban cohort’, *Statistical Communications in Infectious Diseases* **4**(1).
- Romero-Severson, E., Volz, E., Koopman, J., Leitner, T. and Ionides, E. (2015), ‘Dynamic variation in sexual contact rates in a cohort of HIV-negative gay men’, *American Journal of Epidemiology* **182**, 255–262.
- Shrestha, S., King, A. A. and Rohani, P. (2011), ‘Statistical inference for multi-pathogen systems’, *PLoS Computational Biology* **7**(8), e1002135.
- Vittinghoff, E., Douglas, J., Judon, F., McKiman, D., MacQueen, K. and Buchinder, S. P. (1999), ‘Per-contact risk of human immunodeficiency virus transmission between male sexual partners’, *American Journal of Epidemiology* **150**(3), 306–311.
- Whiteley, N. (2013), ‘Stability properties of some particle filters’, *Annals of Applied Probability* **23**, 2500–2537.
- Winsor, C. P. (1932), ‘The Gompertz curve as a growth curve’, *Proceedings of the National Academy of Sciences of the USA* **18**, 1–8.
- Wood, S. N. (2010), ‘Statistical inference for noisy nonlinear ecological dynamic systems’, *Nature* **466**, 1102–1104.
- Yang, Y., Halloran, M. E., Daniels, M. J., Longini, I. M., Burke, D. S. and Cummings, D. A. T. (2010), ‘Modeling competing infectious pathogens from a Bayesian perspective: Application to influenza studies with incomplete laboratory results’, *Journal of the American Statistical Association* **105**(492), 1310–1322.

Yang, Y., Longini Jr., I. M., Halloran, M. E. and Obenchain, V. (2012), ‘A hybrid EM and Monte Carlo EM algorithm and its application to analysis of transmission of infectious diseases’, *Biometrics* **68**(4), 1238–1249.

S1 Alternative POMP representations of a PanelPOMP

Section 2.1 of the main text developed a partially observed Markov process (POMP) representation of a PanelPOMP, which we call construction R1. The following constructions, R2 and R3, provide two alternative ways to write a PanelPOMP as a POMP.

(R2) For a panel in which each unit is observed over the same time interval, we can write

$$X^{[2]}(t) = (X_1(t), X_2(t), \dots, X_U(t)).$$

This constructs a POMP by concatenating the latent state vectors for each separate unit of the PanelPOMP. The dimension of the resulting latent process increases with the number of panel units, U . Sequential Monte Carlo (SMC) methods struggle with high-dimensional latent processes (Bengtsson et al., 2008). This representation is therefore anticipated to be useful for SMC based methodology only when U is small.

(R3) The latent process for a PanelPOMP model need only be specified at the observation times. Therefore, we can define an equivalent integer-time POMP model,

$$X^{[3]}(u) = (X_{u,0}, X_{u,1}, \dots, X_{u,N_u}).$$

The dynamics in this POMP model are trivial: $X^{[3]}(i)$ is independent of $X^{[3]}(j)$ for $i \neq j \in 1:U$. Due to the ‘curse of dimensionality’ for importance sampling, this representation is useful for SMC based methodology only when all of N_1, \dots, N_U are small. This representation can provide a simple way to apply existing POMP methodology to panel data, and for that reason it was adopted by Romero-Severson et al. (2015).

The only reasons of which we are aware to give preference to R2 or R3 over R1 are small potential gains in conceptual and coding simplicity. However, the scaling difficulties faced by both R2 and R3 make them inappropriate for general-purpose methodology and software based on SMC.

S2 Estimators for the likelihood of a PanelPOMP

Consider $R \geq 2$ independent particle filters, each with $J \geq 1$ particles, which give independent Monte Carlo likelihood estimators $L_u^{(r)}$, $r \in 1:R$, for each unit. We work with a constant parameter value θ and write $\ell_u(\theta) = \ell_u$. The Monte Carlo estimator is unbiased and has finite variance, written as

$$\mathbb{E}[L_u^{(r)}] = \ell_u, \quad \text{Var}[L_u^{(r)}] = \sigma_u^2 < \infty.$$

A corresponding estimator of the full panel likelihood based on replication r is

$$L^{(r)} = \prod_{u=1}^U L_u^{(r)},$$

which has mean and variance given by

$$\mathbb{E}[L^{(r)}] = \ell, \quad \text{Var}[L^{(r)}] = \prod_{u=1}^U \left\{ \sigma_u^2 + \ell_u^2 \right\} - \ell^2.$$

A natural approach to combining the R independent likelihood estimators for estimation of the likelihood of a single panel unit u is

$$\bar{L}_u = \frac{1}{R} \sum_{r=1}^R L_u^{(r)},$$

which has mean and variance given by

$$\mathbb{E}[\bar{L}_u] = \ell_u, \quad \text{Var}[\bar{L}_u] = R^{-1} \sigma_u^2.$$

However, it is not immediately clear how to combine the unit-level likelihood estimators to estimate the likelihood of the entire panel. We consider two estimators,

$$\tilde{L} = \frac{1}{R} \sum_{r=1}^R L^{(r)}, \quad \hat{L} = \prod_{u=1}^U \bar{L}_u.$$

While both estimators are unbiased, \tilde{L} is less efficient than \hat{L} . To see this, consider first their variances,

$$\text{Var}[\tilde{L}] = \frac{1}{R} \left[\prod_{u=1}^U \left\{ \sigma_u^2 + \ell_u^2 \right\} - \ell^2 \right] \quad (\text{S1})$$

$$\begin{aligned} \text{Var}[\hat{L}] &= \mathbb{E} \left[\prod_{u=1}^U \bar{L}_u \right]^2 - \ell^2 \\ &= \prod_{u=1}^U \left\{ \frac{\sigma_u^2}{R} + \ell_u^2 \right\} - \ell^2. \end{aligned} \quad (\text{S2})$$

Expanding the product in (S1) yields

$$\text{Var}[\tilde{L}] = \frac{1}{R} \left[\sum_{k_{1:U} \in \{0,1\}^U} \left\{ \prod_{u=1}^U \sigma_u^{2k_u} \ell_u^{2(1-k_u)} \right\} - \ell(\theta)^2 \right]. \quad (\text{S3})$$

The term ℓ^2 in (S3) cancels with the summand for $k_{1:U} = (0, 0, \dots, 0)$, giving

$$\text{Var}[\tilde{L}] = \sum_{k_{1:U} \in \{0,1\}^U \setminus \{0\}^U} \left\{ \frac{1}{R} \prod_{u=1}^U \sigma_u^{2k_u} \ell_u^{2(1-k_u)} \right\}. \quad (\text{S4})$$

An analogous expression for $\text{Var}[\widehat{L}]$, derived from (S2), is

$$\text{Var}[\widehat{L}] = \sum_{k_{1:U} \in \{0,1\}^U \setminus \{0\}^U} \left\{ \left[\prod_{u=1}^U \frac{1}{R^{k_u}} \right] \prod_{u=1}^U \sigma_u^{2k_u} \ell_u^{2(1-k_u)} \right\}. \quad (\text{S5})$$

Comparing equivalent terms in the sums for (S4) and (S5) we see that, supposing that either variance is strictly positive (which, from the unbiasedness of the likelihood estimator, implies that σ_u^2 and $\ell_u(\theta)$ are strictly positive) and given that $R > 1$,

$$\text{Var}[\widehat{L}] < \text{Var}[\widetilde{L}].$$

For a quantitative comparison of \widetilde{L} and \widehat{L} , consider the situation with constant likelihood, $\ell_u = \ell$, and constant variance, $\sigma_u^2 = \sigma^2$. Then,

$$\text{Var}[\widetilde{L}] = \frac{1}{R} [(\sigma^2 + \ell^2)^U - \ell^{2U}], \quad \text{Var}[\widehat{L}] = \left(\frac{\sigma^2}{R} + \ell^2 \right)^U - \ell^{2U}. \quad (\text{S6})$$

Further, suppose we are interested in the relative likelihood so we can scale to $\ell = 1$. Now, if $R = cU$ for some constant c , then we see from (S6) that $\text{Var}[\widehat{L}]$ is stable as $U \rightarrow \infty$ whereas $\text{Var}[\widetilde{L}]$ increases exponentially.

S3 Graphs for subsets of the polio and contacts data

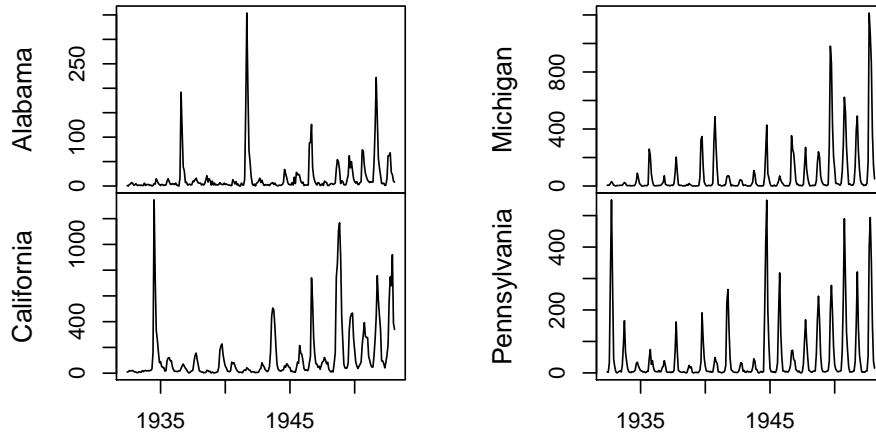


Figure S-1: Selection of 4 time series from the panel dataset from Martinez-Bakker et al. (2015) giving USA monthly of acute paralysis from polio from May 1932 through January 1953 for the 48 continuous US states and Washington D.C. Birth data are missing for South Dakota (before January 1933) and Texas (before January 1934) and so these states were modeled over a reduced time interval. The full data can be accessed from the `panpo1` panelPomp object included in the `panelPomp` package.

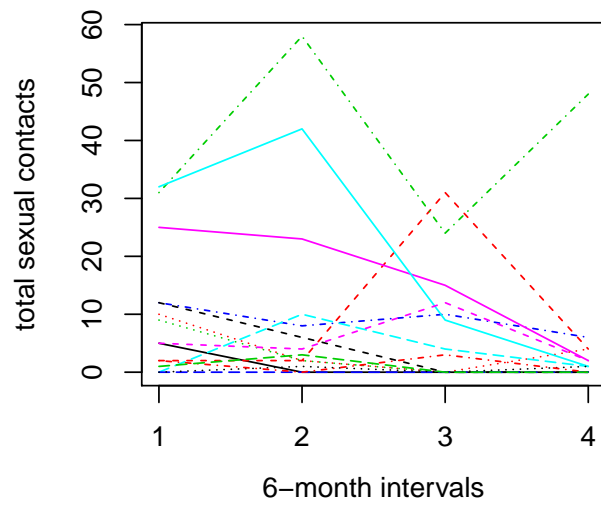


Figure S-2: Sample of 15 time series in the panel dataset from Vittinghoff et al. (1999) on total sexual contacts over four consecutive 6-month periods, for the 882 men having no missing observations. The full data can be accessed from the `pancon` `panelPomp` object included in the `panelPomp` package.

S4 Algorithmic parameters

	Gompertz	polio	polio (MCAP interval)	contacts
J_{pf}	4000	5000	5000	4000
R_{pf}	10	10	10	10
J_{if}	2000	4000	4000	4000
R_{if}	13	19	27	13
M	100	236	236	200
$J_{\text{if,u}}$	1000	6000	6000	–
$R_{\text{pf,u}}$	4	2	3	–
M_{u}	50	118	118	–

Table S-1: Algorithmic parameter values used to produce plots in the main text. J_{pf} particles were used for each of R_{pf} replicated particle filter Monte Carlo log likelihood estimates. These replicates were averaged using \widehat{L} (defined in Section S2). The resulting log likelihood estimates correspond to parameter values with maximum likelihood that were reached initializing the joint step of the panel iterated filtering algorithm at R_{if} different parameter starting values ($\Theta_{1:J}^0$ in the description of the PIF algorithm in the main text), running the algorithm for M iterations. These R_{if} convergence points from the joint step were used to initialize $R_{\text{pf,u}}$ marginal steps with M_{u} iterations and $J_{\text{if,u}}$ particles.

	lower bound	upper bound	σ_0	$\sigma_{\text{u},0}$
r	0.05	0.20	0.00125	–
τ_{u}	0.05	0.20	0.05000	0.05

Table S-2: Starting values, parameter transformations and perturbation specifications for applying PIF to the Gompertz model. The first two columns give the lower and upper bounds of a hyper-rectangle sampled uniformly to generate a value used to initialize all particles $\Theta_{1:J}^0$ for each independent PIF replicate. For the joint maximization, the perturbation sequence used was $\sigma_m = \sigma_0 0.5^{m/50}$. For the marginal maximization, $\sigma_m = \sigma_{\text{u},0} 0.25^{m/50}$ was used instead. These random perturbations were carried out as Gaussian random walks after applying a logarithmic transformation to ensure non-negativity constraints were met.

	lower bound	upper bound	transformation	σ_0	$\sigma_{u,0}$
σ_{dem}	0.0	0.50	log	0.02	–
ψ	0.0	0.10	log	0.02	–
τ	0.0	0.10	log	0.02	–
$b_{u,1}$	-2	8.00	–	0.02	0.02
$b_{u,2}$	-2	8.00	–	0.02	0.02
$b_{u,3}$	-2	8.00	–	0.02	0.02
$b_{u,4}$	1.0	11.0	–	0.02	0.02
$b_{u,5}$	-2	8.00	–	0.02	0.02
$b_{u,6}$	-2	8.00	–	0.02	0.02
$\sigma_{u,\text{env}}$	0.0	1.00	log	0.02	0.02
$\tilde{S}_{u,0}^O$	0.0	1.00	logit	0.10	0.10
$\tilde{I}_{u,0}^O \times 10^4$	0.0	4.00	logit	0.20	0.20

Table S-3: Starting values, parameter transformations and perturbation specifications for applying PIF to the polio model. The first two columns give the lower and upper bounds of a hyper-rectangle sampled uniformly to generate a value used to initialize all particles $\Theta_{1:J}^0$ for each independent PIF replicate. For the joint maximization, the perturbation sequence used was $\sigma_m = \sigma_0 0.5^{m/50}$. For the marginal maximization, $\sigma_m = \sigma_{u,0} 0.25^{m/50}$ was used instead. Some of these random perturbations were carried out as Gaussian random walks after applying a transformation to ensure that non-negativity and unit-interval constraints were met, and these transformations are given in the third column.

	lower bound	upper bound	transformation	σ_0
μ_X	0.80	3.00	log	0.01
σ_X	1.40	5.00	log	0.01
μ_D	1.80	7.00	log	0.01
σ_D	2.00	8.50	log	0.01
α	0.70	0.99	logit	0.01

Table S-4: Starting values, parameter transformations and perturbation specifications for applying PIF to the contacts model. The first two columns give the lower and upper bounds of a hyper-rectangle sampled uniformly to generate a value used to initialize all particles $\Theta_{1:J}^0$ for each independent PIF replicate. For the joint maximization, the perturbation sequence used was $\sigma_m = \sigma_0 0.5^{m/50}$. These random perturbations were carried out as Gaussian random walks after applying the transformations in the third column to ensure that non-negativity and unit-interval constraints were met. Marginal maximization was not applicable in this example since all parameters were shared.

Supplementary References

- Bengtsson, T., Bickel, P. and Li, B. (2008), Curse-of-dimensionality revisited: Collapse of the particle filter in very large scale systems, *in* T. Speed and D. Nolan, eds, ‘Probability and Statistics: Essays in Honor of David A. Freedman’, Institute of Mathematical Statistics, Beachwood, OH, pp. 316–334.
- Martinez-Bakker, M., King, A. A. and Rohani, P. (2015), ‘Unraveling the transmission ecology of polio’, *PLoS Biology* **13**(6), e1002172.
- Romero-Severson, E., Volz, E., Koopman, J., Leitner, T. and Ionides, E. (2015), ‘Dynamic variation in sexual contact rates in a cohort of HIV-negative gay men’, *American Journal of Epidemiology* **182**, 255–262.
- Vittinghoff, E., Douglas, J., Judon, F., McKimman, D., MacQueen, K. and Buchinder, S. P. (1999), ‘Per-contact risk of human immunodeficiency virus transmission between male sexual partners’, *American Journal of Epidemiology* **150**(3), 306–311.